Korean J. Chem. Eng., 39(9), 2465-2473 (2022)
DOI: 10.1007/s11814-022-1144-x

pISSN: 0256-1115
eISSN: 1975-7220

Polyphenylsulfone/polyethylene glycol hexadecyl ether blend membranes with enhanced surface hydrophilicity for high-performance nanofiltration of dye solution

Bahareh Rastegar, Ehsan Saljoughi†, Seyed Mahmoud Mousavi, and Shirin Kiani

Chemical Engineering Department, Faculty of Engineering, Ferdowsi University of Mashhad, Mashhad, Iran
(*Received 27 August 2021 • Revised 31 March 2022 • Accepted 10 April 2022*)

Abstract−Hydrophilic membranes composed of polyphenylsulfone (PPSU)/polyethylene glycol hexadecyl ether (Brij-58), with noticeable properties and performance in the filtration of dye solution, were prepared for the first time. Scanning electron microscopy (SEM) images were utilized to examine the morphology of the obtained membranes. Attenuated total reflection Fourier-transform infrared (ATR-FTIR) spectra, water contact angle, water uptake capacity, and tensile properties of the membranes confirmed that Brij-58 remained in the structure of the obtained membranes due to the high molecular weight of the additive. Higher water contact angle and water uptake capacity obtained with increasing the Brij-58 concentration showed enhanced membrane hydrophilicity. The addition of Brij-58 and increasing its concentration was followed by a constant increase in pure water flux (PWF) and antifouling property of the membrane. According to the results, the incorporation of 10 wt% Brij-58 into the polymeric solution contributed to almost 54-fold higher water flux and approximately 36% higher flux recovery ratio (FRR), while the rejection of disperse blue was only slightly reduced.

Keywords: Membrane, Surface Hydrophilicity, Polyphenylsulfone, Brij-58, Disperse Blue, Fouling

INTRODUCTION

Today, the worldwide shortage of water has caused many problems [1], along with water quality issues also rising in many areas of the world [2]. Therefore, the treatment of wastewaters produced from different industries can significantly help to address the problems associated with the mentioned problems.

Among various methods for water treatment, membrane separation process is a perfect option for industrial wastewater treatment because it has advantages such as selective separation and purification without adding chemicals [3]. Industrial membranes are made from inorganic or organic (polymeric) materials; however, polymeric membranes are used widely because of their low cost and high flexibility [4,5].

A wide variety of polymers are used for membrane preparation, including polyvinylidene fluoride (PVDF) [6,7], polyacrylonitrile (PAN) [8,9], polyimide (PI) [10,11], polysulfone (PSU) [12, 13], polyethersulfone (PES) [14,15], and polyphenylsulfone (PPSU) [16]. PPSU is a good option for membrane preparation among different polymers since it is produced easily; also, this polymer has long-term thermal stability because of the stable structure of diphenyl-sulfonyl resonance [17]. Other advantages of PPSU are its high strength and stiffness and high resistance to environmental stress cracking [18]. This amorphous polymer has a high glass transition temperature of about 220-222 °C [19]. It is more resistant against acids and bases, ionic surfactants, aliphatic amines, alcohols, and glycols, compared to PSU and PES [20]. However, despite these advantages, PPSU is a polymer with low hydrophilicity, limiting its application in aqueous filtration [21]. Consequently, the hydrophilicity improvement of PPSU membranes is required for enhancing their performance.

Methods applied in improving the hydrophilicity of PPSU membranes are generally classified into two groups: surface modification and bulk modification. Zhong et al. [22] studied the improvement of sulfonated PPSU (sPPSU) membrane surface via UV-induced grafting of [2-(methacryloyloxy) ethyl] trimethyl ammonium chloride and diallyldimethylammonium chloride. They found that the water contact angle was reduced with monomer grafting, but pure water permeability was also reduced because of pore size reduction due to chemical bonds. Reports on improving the bulk of PPSU membranes can be classified into monomer or polymer modification with $-SO_3H$ group [23] as well as $-SO_3H$ and $-NO_2$ groups [24], blending with hydrophilic polymers [25], and the addition of hydrophilic compounds such as nanoparticles [21,26-28] and surfactants [29-32].

Among various methods for hydrophilicity improvement of membranes, the addition of hydrophilic materials to the casting solution has attracted much attention, mainly due to the ease of process as well as the simultaneous formation and modification of the membrane. As mentioned above, one of the membrane improvement strategies is the use of surfactants, which have a hydrophilic head and a hydrophobic tail in their structure. It was reported that a surfactant added to the polymeric casting solution might leach out partly into the coagulation bath during membrane preparation and thus act as a pore-forming agent. At the same time, a residual amount remains in the membrane structure and affects the properties of the final membrane [33]. Kiani et al. [34] blended PPSU with two different polyethylene glycols (PEGs). Their results

†To whom correspondence should be addressed.
E-mail: saljoughi@um.ac.ir

revealed a lower water contact angle, higher water flux, and increased flux recovery with PEG addition. The influence of other surfactants such as polyvinylpyrrolidone (PVP), PEG, and tween-80 on the hydrophilicity enhancement of PPSU membranes was also reported by Liu et al. [32].

Polyethylene glycol hexadecyl ether (Brij-58) is a significantly hydrophilic surfactant whose positive effect on the hydrophilicity of PSU [35] and PVDF [36] membranes were reported earlier. Therefore, due to the excellent results obtained by the addition of Brij-58 to polymeric membranes, and according to the fact that the effect of blending PPSU with this surfactant has not been investigated before, Brij-58 was used in this research as a hydrophilic additive with the aim of hydrophilicity improvement of PPSU membrane. Several characterizations were performed to study the influence of the additive on the membrane properties. The performance of the membranes in the filtration of aqueous media was also investigated.

MATERIALS AND METHODS

1. Materials

Polyphenylsulfone (PPSU, average MW=50,000 g/mol) was purchased from Solvay Advanced Polymers (Belgium). N-methyl-2-pyrrolidone (NMP) (purity=99.5%) was provided by Daejung (Korea). Polyethylene glycol hexadecyl ether (Brij-58, average MW=1,124 g/mol) with the hydrophilic-lipophilic balance (HLB) of 16 was supplied by Sigma-Aldrich. Bovine serum albumin (BSA, average MW=66.5 kDa) was obtained from Equitech-Bio. Disperse Blue 106 (MW=335.4 g/mol) was provided by a textile factory.

2. Membrane Preparation

PPSU and PPSU/Brij-58 membranes were prepared by the immersion-precipitation method. PPSU solution was obtained by stirring 17 wt% PPSU in the solvent (NMP) at room temperature for 24 h. Also, to obtain the PPSU/Brij-58 blend solutions, the specified amount of Brij-58 (2, 4, 6, 8, and 10 wt% of the final solution) was dissolved in NMP for 24 h. Then PPSU (17 wt% of the final solution) was added with continued stirring for another 24 h. The composition of the casting solutions is shown in Table 1.

After degassing for 24 h, the polymeric solution was cast on a smooth plate using a film applicator with a gap of 250 μm. The obtained polymeric film was immersed in a 10 °C distilled water coagulation bath. After ten minutes, the formed membranes were transferred to another water bath at room temperature and left there for one day. The resultant membranes were used in the wet state for the filtration tests or dried overnight at room temperature to be characterized further.

Table 1. Composition of polymeric solutions utilized for membrane casting

Membrane code	PPSU (wt%)	Brij-58 (wt%)	NMP (wt%)
M0	17	0	83
M2	17	2	81
M4	17	4	79
M6	17	6	77
M8	17	8	75
M10	17	10	73

3. Characterization

Membrane morphology was studied using LEO 1450 VP (Germany) scanning electron microscopy (SEM) equipment. Prior to imaging, the samples were freeze-fractured and then coated with Au. Membrane thickness was obtained by analyzing the SEM images using the ImageJ software. Using ImageJ software requires the adjustment of the scale in the first step. Then, membrane thickness was measured at three different points of the cross-sectional SEM image, and the average value was reported.

To determine the membrane porosity, the wet membrane sample was weighed after removing the water droplets from its surface (W_w, g). Then the membrane thickness in its wet state was measured in three points using the Insize digital micrometer, and the average thickness was used as the thickness of the wet membrane (δ, cm). The mentioned membrane was then dried at ambient temperature for one week. Finally, the dried membrane sample was weighed again (W_d, g), and membrane porosity was obtained via the equation below [37]:

$$\varepsilon(\%) = \frac{W_w - W_d}{\rho_w A \delta} \times 100 \quad (1)$$

where A and ρ_w are the membrane area in the wet state (cm^2) and the density of pure water (0.997 g/cm^3), respectively. Since the membrane is swollen in its wet state, applying the dimensions of the swollen sample would offset the overestimation of membrane porosity.

The presence of Brij-58 in the membrane structure was confirmed via the attenuated total reflection Fourier-transform infrared (ATR-FTIR) spectroscopy using the Thermo Nicolet Avatar 370 equipment.

The water contact angle of the membrane surface was measured by taking the images of 5-7 droplets of distilled water on the membrane surface using an Olympus SZH10 Stereo microscope. For each membrane, three samples were examined, and the average of water contact angles was recorded.

To determine the amount of water uptake by the membrane, a completely dried membrane sample was weighted (W_0, g) and then immersed in distilled water for 24 h. Membrane samples were weighed again after the removal of water droplets from its surface (W, g), and water content was determined according to the equation below [38]:

$$WC(\%) = \frac{W - W_0}{W_0} \times 100 \quad (2)$$

Tensile properties were investigated with a SANTAM universal testing machine (STM-20, Iran) at room temperature. Dimensions of membrane samples were 70×10 mm with 50 mm gauge length, and all the membrane samples were stretched at 12.5 mm/min. For each membrane, the tensile test was repeated three times.

4. Filtration Experiments

Fig. 1 shows a schematic of the filtration setup. For the investigation of pure water flux (PWF), the membrane sample (effective area=15.89 cm^2) was put in the cross-flow membrane module. The feed tank was filled with 3 L distilled water. Feed water passed across the membrane surface for three hours at the transmembrane pressure (TMP) of 5 bar to induce pre-compaction. After that, PWF was measured at TMP of 5 bar every 15 min for membranes with

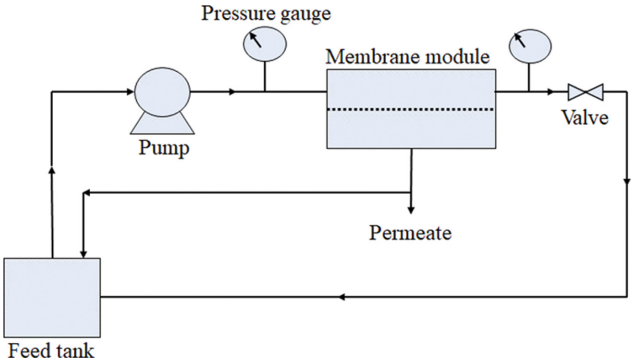

Fig. 1. Schematic of the filtration setup.

high flux (M6 to M10 samples) and every 30 min for membranes with low flux (M0 to M4 samples) until two equal PWF values were obtained successively. PWF was determined using the equation below [34]:

$$\text{Flux} = \frac{V}{A_{eff} \cdot \Delta t} \tag{3}$$

where V, A_{eff}, and Δt are the permeate volume (L), the effective membrane area (m^2), and the sampling time (h), respectively.

One of the methods for investigating membrane tendency to fouling is the determination of flux recovery ratio (FRR) after the filtration of an aqueous solution containing BSA. For this purpose, after PWF measurement (J_0), the feed tank was filled with an aque-

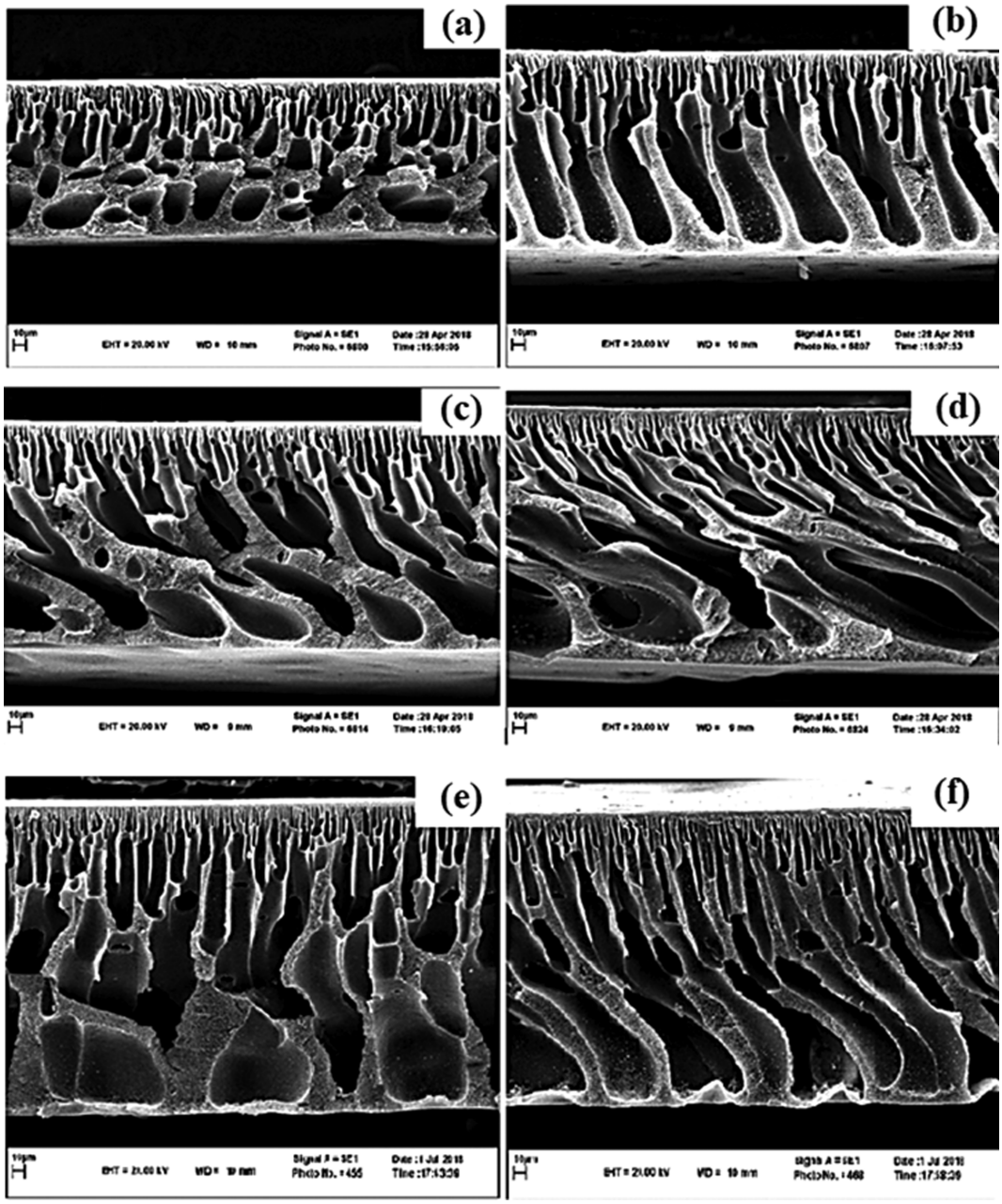

Fig. 2. Cross-sectional SEM images of the membranes: (a) M0, (b) M2, (c) M4, (d) M6, (e) M8, (f) M10.

ous solution of BSA with a concentration of 1 g/L. The BSA solution passed across the membrane surface at the TMP of 5 bar until the permeate flux became constant. Next, the filtration module and the membrane were washed for 30 min with distilled water to remove the protein molecules, which reversibly accumulated on the membrane surface during filtration. PWF of the membrane was measured again (J_1), and FRR was calculated using the equation below [39]:

$$FRR\ (\%) = \frac{J_1}{J_0} \times 100 \quad (4)$$

To investigate the separation performance of prepared membranes, filtration of an aqueous solution of 20 ppm disperse blue was conducted. After the measurement of PWF, the filtration of the dye solution was performed at the TMP of 5 bar, and permeate volume was determined at specified time intervals depending on the membrane flux until a steady flux was achieved. Then, the feed and permeate were sampled. The concentration of disperse blue in the samples was analyzed using a UV-Vis spectrophotometer (SP-UV 300 SRB, Germany) at 588 nm. The following equation was applied to calculate the dye rejection (R) [40]:

$$R\ (\%) = \left(1 - \frac{C_p}{C_F}\right) \times 100 \quad (5)$$

where C_p and C_F are disperse blue concentrations in the permeate and feed, respectively.

RESULTS AND DISCUSSION

1. SEM

The morphology of PPSU/Brij-58 membranes and the neat PPSU membrane was investigated using SEM images. The cross-sectional morphology of the prepared membranes is provided in Fig. 2. Fig. 3 shows the variation in membrane porosity and thickness with increasing Brij-58 concentration in the casting solution.

According to Fig. 2, all the membranes had an asymmetric structure in their cross-section, including a thin dense skin on a porous support. It is known that during solvent and nonsolvent exchange, the incompatibility of water and polymer causes the polymer molecules to be driven away and, thus, contributes to the formation of pores in the final membrane structure [35,36]. The SEM images reveal that adding Brij-58 to the casting solution up to 6 wt%, the apparent porosity, and thickness increased significantly. This observation is in agreement with Fig. 3. An increase in porosity and thickness of PPSU membranes in the presence of Brij-58 can be attributed to the hydrophilicity of this additive that led to the acceleration of solvent and nonsolvent exchange in the water bath. Saljoughi et al. [35] and Nikoee et al. [36] reported similar results on the addition of Brij-58 to PSU and PVDF membrane casting solutions, respectively.

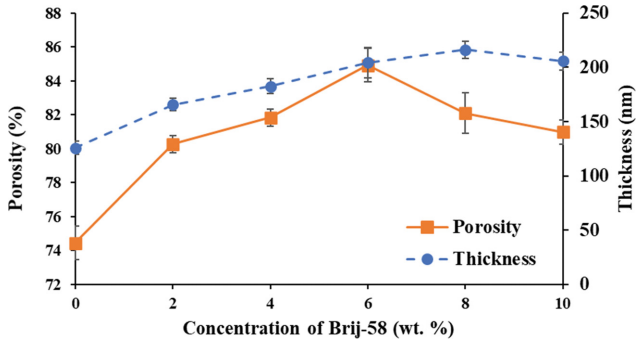

Fig. 3. Thickness and porosity of the PPSU and PPSU/Brij-58 membranes.

Concerning Figs. 2 and 3, M8 and M10 membranes underwent a drop in their porosity. This reduction in porosity, which happened at high concentrations of Brij-58, can be related to the increased viscosity of the casting solution in the presence of the additive, which was intensified at 8 and 10 wt% Brij-58 and decreased the speed of solvent and nonsolvent exchange. This phenomenon overcame the pore-forming effect of the hydrophilic additive and led to porosity reduction. This observation (increase and then decrease in porosity with the addition of hydrophilic additives) was reported for PPSU/PEG [31], PSU/Brij-58 [35], and PVDF/Brij-58 [36] membranes.

Although Figs. 2 and 3 reveal a drop in the porosity of the M8 membrane, the thickness of this membrane increased. The ironically higher membrane thickness at lower porosity might be due to the dominant effect of increased solid content over the effect of less membrane free volume [41]. However, a further increase in Brij-58 concentration (10 wt%) was followed by the decrease in the membrane thickness because of the lower membrane porosity and thus its lower free volume.

2. Chemical Structure

In Fig. 4, the ATR-FTIR spectra corresponding to the pure PPSU membrane and the membranes improved with 6 and 10 wt% Brij-58 are presented. The peaks at 1,294 and 1,323 cm^{-1} in the spectrum of the pure PPSU membrane are related to the $S(=O)_2$ group [31]. In addition, peaks at 1,484 and 1,585 cm^{-1} are related to the C=C group [31].

In membranes containing Brij-58 additive, the presence of Brij-58 in the membrane structure was confirmed by the appearance of a peak at about 3,500 cm^{-1} (O-H group) and also two peaks at 2,856 and 2,923 cm^{-1} (C-H group) [42]. It can be seen that increasing the additive concentration increased the intensity of the mentioned peaks. The obtained results reveal that the utilized additive remained in the membrane structure during the membrane formation. Thus, it not only had the role of a pore former during membrane formation, but it also affected the hydrophilicity of the resultant blend membranes.

3. Water Contact Angle

The water contact angle was determined for the PPSU and PPSU/Brij-58 membranes, and the results are presented in Fig. 5. As can be seen, the highest water contact angle (77.6°), i.e., the lowest hydrophilicity, was related to the pure PPSU membrane, and the addition of Brij-58 brought about lower water contact angles. Moreover, lower contact angles were obtained with a higher additive concentration. The lowest water contact angle (41.6°), i.e., the highest hydrophilicity, is assigned to the M10 membrane sample. The improved hydrophilicity of the membranes in the presence of Brij-58 can be attributed to the O-H group that is available in the Brij-58 structure [36].

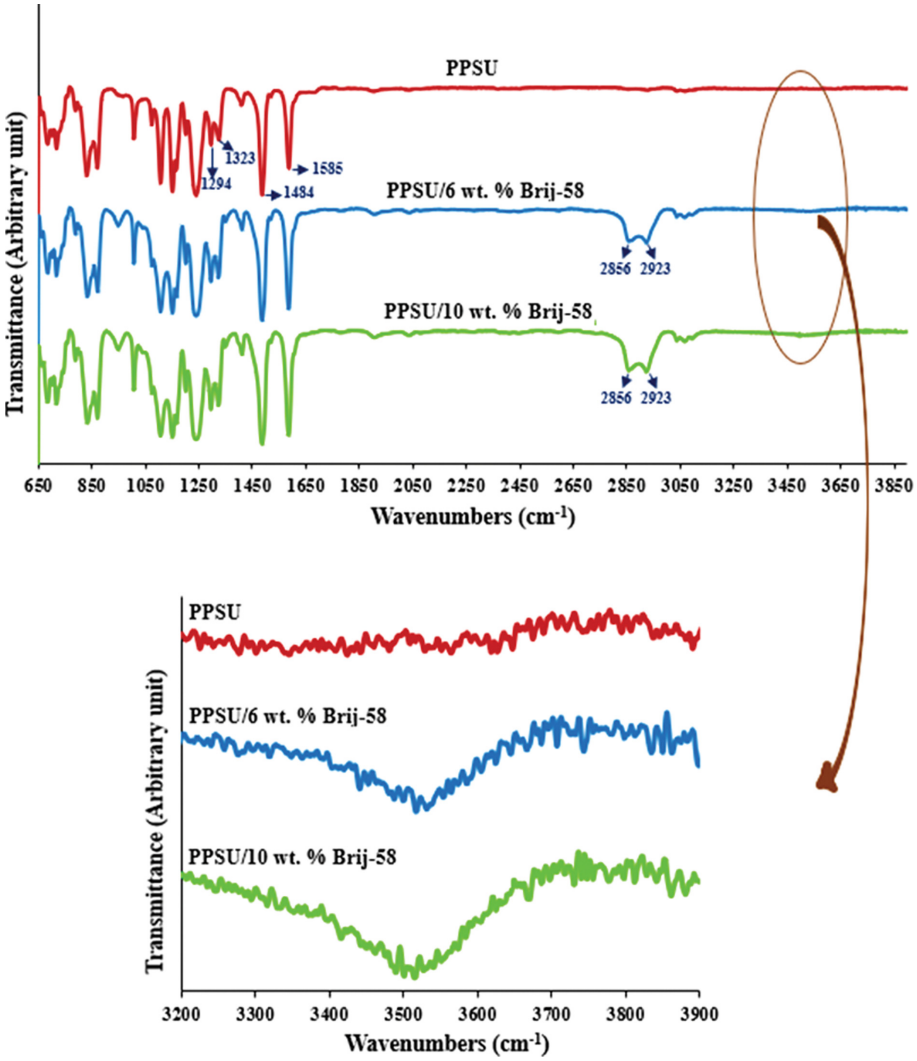

Fig. 4. ATR-FTIR spectra of the PPSU and PPSU/Brij-58 membranes.

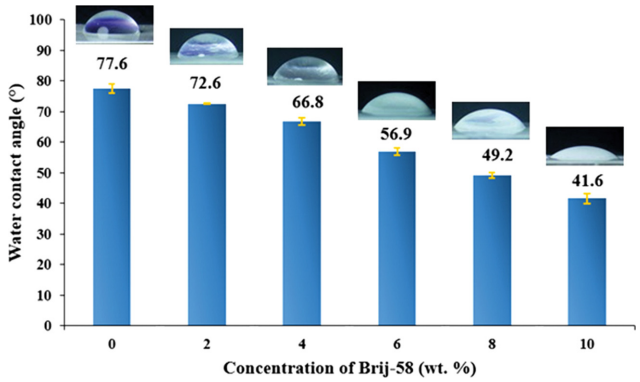

Fig. 5. Water contact angles of the PPSU and PPSU/Brij-58 membranes.

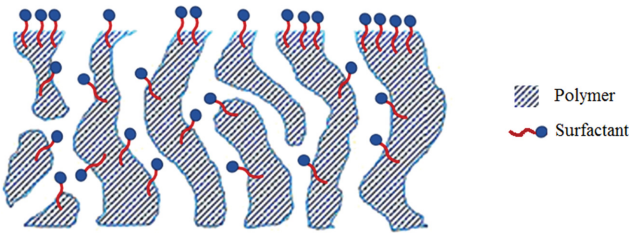

Fig. 6. Schematic representation of the PPSU/Brij-58 membrane structure.

Fig. 6 is a schematic representation of the PPSU/Brij-58 membrane after immersion-precipitation. As shown, it seems that during the immersion-precipitation of the polymeric solution in the coagulation bath, the Brij-58 molecules are ordered in such a way that the hydrophilic head of Brij-58 is arranged on the polymer-water interface on the membrane surface and areas where water penetrates (membrane pores). The water affinity of this hydrophilic tail results in the presence of a high concentration of hydrophilic groups in the mentioned areas, and thus the membrane hydrophilicity is improved significantly [37,48].

Note that the results of ATR-FTIR spectroscopy (section 3.2) previously confirmed that Brij-58 remained in the membrane struc-

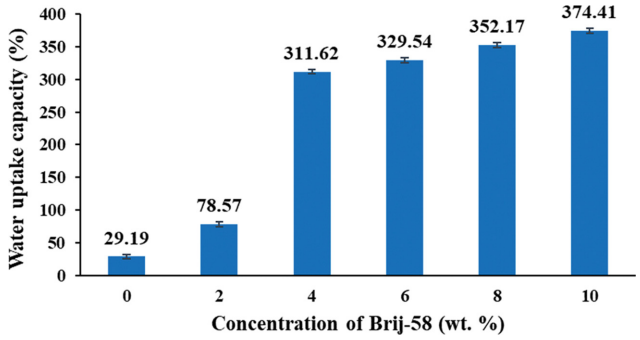

Fig. 7. Water uptake capacity of the PPSU and PPSU/Brij-58 membranes.

ture. Regarding the hydrophilicity of Brij-58 and its high tendency to water, this question arises: How did Brij-58 remain in the membrane structure? The high molecular weight of Brij-58 explains the answer. As shown in Fig. 6, the molecule of this additive has a relatively long hydrophobic tail, which entangles with the PPSU polymeric chains and prevents the additive from leaving the membrane structure. Other researchers that utilized high-molecular-weight surfactants as additives proved the presence of residual additive in the resultant membrane structure, too [31].

4. Water Uptake

The amount of water uptake by the membranes prepared in this work is presented in Fig. 7. As can be seen, the pure PPSU membrane shows 29.2% water uptake, which increased in the presence of the hydrophilic additive. The presence of more Brij-58 in the membranes augmented the water content. Thus the water uptake of the membrane obtained by 10 wt% Brij-58 achieved the highest value (374.4%) among the other membranes. According to the literature, water uptake is affected by membrane porosity and hydrophilicity [31]. In detail, higher membrane porosity and increased membrane hydrophilicity are beneficial to the degree of water uptake [31].

According to Fig. 7, the initial increase in the water content, which happened in M2, M4, and M6 samples, can be related to the simultaneous impact of increased porosity and hydrophilicity of the membranes. Nevertheless, a further increase in the water content using more Brij-58 in the casting solution can only be related to the higher hydrophilicity of the membrane since the membrane porosity dropped in the corresponding membranes. Therefore, in the present case, if the hydrophilic additive (Brij-58) had not been retained in the membrane structure and had left the polymeric solution during solidification in the coagulation bath, the water uptake capacity would have been affected only by the membrane porosity and an increasing and then decreasing trend would have been observed in the water content. However, the obtained results confirm the presence of residual additive in the samples and are in agreement with the results of previous sections. Kiani et al. [31] observed similar results with the addition of PEG 20,000 to the PPSU membrane. In their paper, water uptake increased despite the reduction in membrane porosity and was attributed to the improved hydrophilicity of the membrane.

Note that the addition of 4 wt% Brij-58 contributed to a sharp increase in water content. This observation can be explained as follows: some Brij-58 molecules leave the polymeric solution during its phase inversion, while the entanglements of polymer and Brij-58 chains hold a residual amount of Brij-58 in the membrane structure. With the increase in solution viscosity, chain entanglement is augmented and the residual Brij-58 increases. Therefore, the membrane prepared by 4 wt% Brij-58 contains significantly more hydrophilic additive compared to the membrane prepared by 2 wt% Brij-58, not only because of the higher amount of the additive in the solution, but also due to the entrapment of more residual Brij in the membrane structure.

5. Mechanical Properties

Stress-strain curves obtained for PPSU and PPSU/Brij-58 membranes are presented in Fig. 8. The numerical values of mechanical properties derived from Fig. 8 are shown in Table 2.

According to the data presented in Table 2, it is evident that the elastic modulus and tensile strength of the membranes are generally reduced in the presence of Brij-58 and also with increasing its concentration. A different trend was observed for elongation at break. With an initial increase in Brij-58 loading, elongation at break was reduced from 29.8% (M0 sample) to 13.1% (M4 sample), but

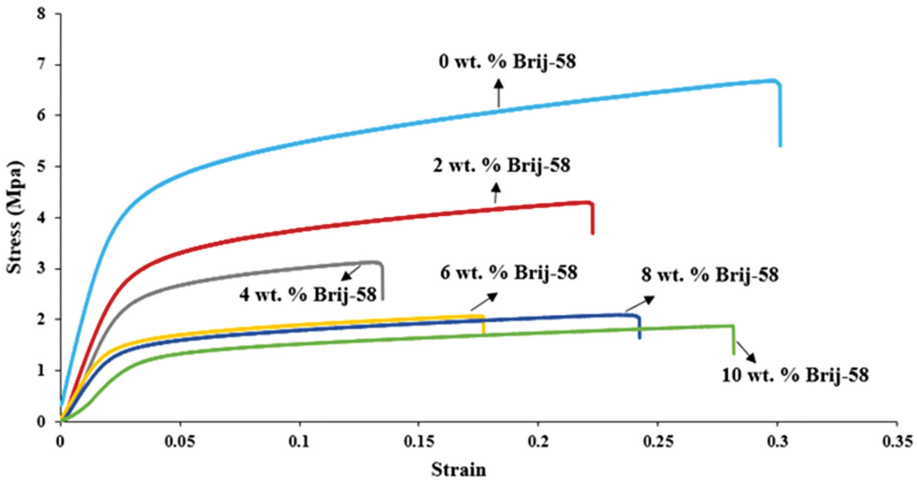

Fig. 8. Stress-strain curves obtained for the PPSU and PPSU/Brij-58 membranes.

Table 2. Tensile properties of membranes

Membrane	Elastic modulus (MPa)	Tensile strength at break (MPa)	Elongation at break (%)
M0	179.2±4.3	6.7±0.5	29.8±1.3
M2	123.4±5.7	4.3±0.2	22.0±2.4
M4	92.6±2.4	3.9±0.2	13.1±1.9
M6	79.5±2.0	2.1±0.2	17.5±1.5
M8	71.1±3.1	2.1±0.2	23.4±2.1
M10	61.3±4.0	1.9±0.1	28.1±1.8

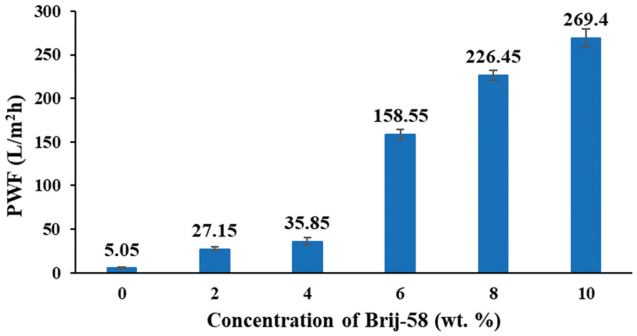

Fig. 9. PWF of the PPSU and PPSU/Brij-58 membranes.

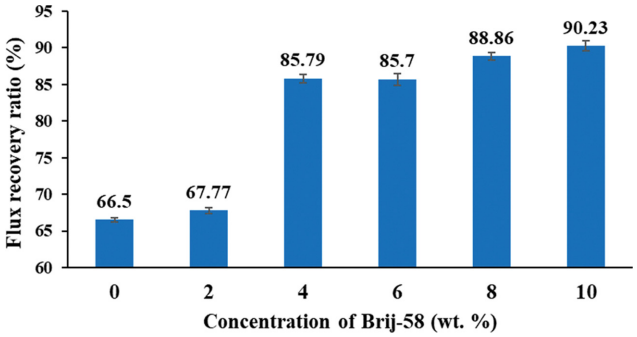

Fig. 10. Flux recovery ratio of the PPSU and PPSU/Brij-58 membranes.

with further increase in additive concentration, elongation at break increased to 28.1% (M10 sample).

The changes in membrane mechanical properties can be explained considering the variation in membrane porosity and the plasticizing effect of Brij-58. Results of previous studies show that all the three mentioned tensile properties decrease with an increase in membrane porosity [37,43]. It was shown that the membrane porosity was increased in M2, M4, and M6 samples, while it was reduced using a higher concentration of the additive. Thus, the declining trend of tensile properties in M2 and M4 samples can be attributed to the porosity improvement of these membranes. However, the mechanical properties of M6, M8, and M10 membrane samples were influenced mainly by another factor: the higher flexibility of polymeric chains in the presence of plasticizers (Brij-58) [44]. The presence of additives with a plasticizing effect is detrimental to elastic modulus and tensile strength, while it is beneficial to elongation at break [45]. The determined tensile properties again confirm that Brij-58 remained in the membrane structure since it affected the mechanical properties.

6. PWF

The steady flux of pure water using various additive concentrations in the polymeric solution is shown in Fig. 9. As seen, with the incorporation of Brij-58 into the PPSU membrane structure and increasing its concentration, PWF increased due to the simultaneous effect of porosity and hydrophilicity [46]. Hydrophilicity improvement is beneficial to PWF [47]. In addition, with an increase in porosity, the resistance towards the passage of water molecules is reduced and, as a result, PWF increases [48]. SEM imaging and porosity measurement results revealed that the membrane porosity was increased with increasing Brij-58 concentration to 6 wt% and then was decreased using higher concentrations of additive. Also, according to the results of water contact angle and water uptake measurements, the hydrophilicity of membranes increased with increasing the additive concentration. So, the higher PWF provided by M2, M4, and M6 samples can be due to the simultaneous effect of hydrophilicity and porosity. In addition, despite the falling trend of the porosity of M8 and M10 membranes, their hydrophilicity enhancement had a positive impact on water flux and resulted in a continuous increase of PWF.

7. Antifouling Property

Along with the filtration process, the pollutants either enter membrane pores and block them or accumulate on its surface. This phenomenon, called fouling, causes flux reduction and reduces the useful life of the membrane. To address membrane fouling, the surface hydrophilicity of the membrane can be modified to lower the affinity of the pollutants to the membrane surface [23].

To evaluate the antifouling property of membranes, flux recovery ratio (FRR) as the criterion of membrane resistance against the irreversible fouling was studied using bovine serum albumin (BSA), and the results are in Fig. 10. Generally, the hydrophilicity of the membrane influences the FRR value [49]. Researchers have reported that higher membrane hydrophilicity improves its resistance against fouling.

According to Fig. 10, with increasing the additive concentration from 0 to 10 wt%, FRR was increased continuously from 66.5% to 90.2%. This significant increase in the FRR value shows the positive impact of Brij-58 hydrophilicity on the antifouling property of the PPSU membrane.

8. Filtration of Disperse Blue Solution

The effect of Brij-58 additive in PPSU membranes on the permeate flux and rejection of disperse blue is shown in Fig. 11. As shown, permeate flux followed the same trend as that of the PWF. Thus the explanation given for the variation of PWF with additive

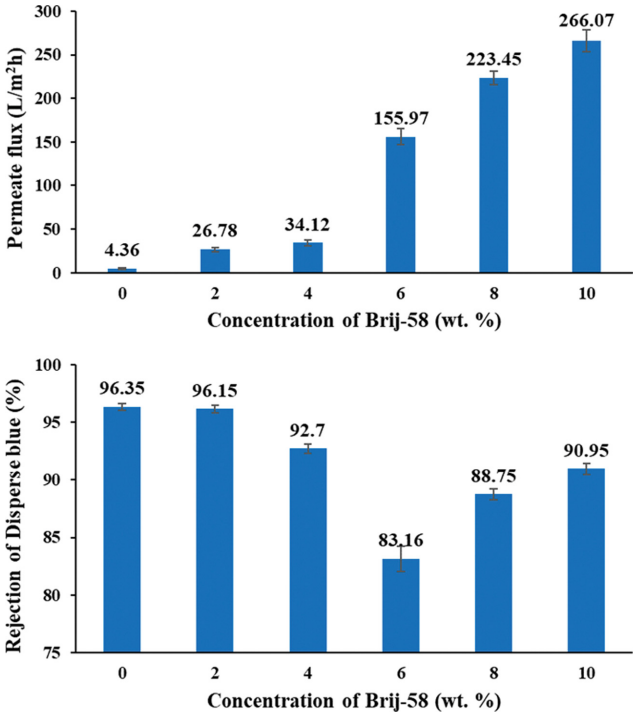

Fig. 11. Permeate flux and rejection of disperse blue using the PPSU and PPSU/Brij-58 membranes.

concentration applies here again. Based on the results, dye rejection was reduced from 96.3% to 83.2% with increasing additive concentration from 0 to 6 wt%, but a higher amount of Brij-58 boosted the rejection value to about 90.9% (M10 sample). Generally, the change in dye rejection is influenced by both membrane porosity and hydrophilicity. Obviously, by increasing the porosity of the membrane, the rejection percent of feed particles is decreased. In contrast, improved membrane hydrophilicity enhances the passage of water molecules and, as a result, increases the solute rejection [33,50].

According to the results, the initial falling trend of dye rejection (M0 to M6 samples) can be related to the rising trend of porosity in the corresponding membranes. However, when higher additive concentration was utilized, the reduced porosity and enhanced hydrophilicity of the resultant membranes favored the dye rejection.

In summary, although the pure PPSU membrane exhibited the highest rejection of disperse blue because of its low porosity, this high dye removal was achieved with very low water flux and much intensive fouling. Indeed, it was shown that the M10 membrane had almost 54-fold higher water flux and approximately 36% higher FRR than the pure PPSU sample, while the rejection of disperse blue was only 5.6% lower in the former.

CONCLUSIONS

PPSU membranes blended with Brij-58 hydrophilic additive were prepared and utilized to remove Disperse blue from its aqueous solution. SEM imaging and porosity measurement indicated that membranes with higher porosity were formed with the increase in the additive loading up to a specific amount, while raising the additive concentration further caused the porosity reduction of membranes. The ATR-FTIR spectra revealed that Brij-58 remained in the membrane structure after the immersion-precipitation and thus affected the membrane hydrophilicity. The presence of Brij-58 in the membrane structure was also confirmed through the increased water contact angles, as well as the higher water uptake capacity of the membranes prepared using higher additive concentrations. Brij-58 influenced the tensile property and filtration performance of the obtained membranes.

The incorporation of Brij-58 into the polymeric solution increased the PWF, and the higher additive concentration resulted in higher PWF values. The investigation of antifouling using the BSA solution showed that the FRR value and, thus, the antifouling properties improved as the additive concentration increased. However, dye rejection during the filtration of an aqueous solution of Disperse blue showed a decrease and then an increase with increasing the additive concentration. Incorporation of 10 wt% Brij-58 into the polymeric solution led to the formation of a membrane with a significantly high PWF (269.4 L/m^{2}h), high resistance against fouling (FRR of 90.2%), and proper dye rejection (90.9%). Although the pure PPSU membrane showed the highest rejection of disperse blue, this high dye removal was achieved with very low water flux and much intensive fouling. However, the incorporation of 10 wt% Brij-58 contributed to almost 54-fold higher water flux and approximately 36% higher FRR than the pure PPSU sample, while the rejection of disperse blue was only 5.6% lower in the former.

NOMENCLATURE

A : membrane area in the wet state [cm^2]
A_{eff} : effective membrane area [m^2]
ATR-FTIR : attenuated total reflection Fourier-transform infrared
Brij-58 : polyethylene glycol hexadecyl ether
BSA : bovine serum albumin
C_f : dye concentration in the feed [ppm]
C_p : dye concentration in the permeate [ppm]
FRR : flux recovery ratio [%]
HLB : hydrophilic-lipophilic balance
J_0 : pure water flux before BSA filtration [L/m^{2}h]
J_1 : pure water flux after BSA filtration [L/m^{2}h]
NMP : N-methyl-2-pyrrolidone
PAN : polyacrylonitrile
PEG : polyethylene glycol
PES : polyethersulfone
PI : polyimide
PPSU : polyphenylsulfone
PSU : polysulfone
PVDF : polyvinylidene fluoride
PVP : polyvinylpyrrolidone
PWF : pure water flux [L/m^{2}h]
R : rejection [%]
SEM : scanning electron microscopy
sPPSU : sulfonated polyphenylsulfone
Δt : filtration time [h]
TMP : transmembrane pressure [bar]
V : permeate volume [L]

W : weight of the membrane sample after immersion in water [g]
W_0 : weight of the membrane sample before immersion in water [g]
WC : water content [%]
W_d : weight of the dry membrane sample [g]
W_w : weight of the wet membrane sample [g]
ε : membrane porosity [%]
δ : thickness of the membrane in the wet state [cm]
ρ_w : density of pure water [g/cm^3]

REFERENCES

1. W. J. Cosgrove and D. P. Loucks, *Water Resour. Res.*, **51**, 4823 (2015).
2. M. T. H. van Vliet, M. Flörke, J. A. Harrison, N. Hofstra, V. Keller, F. Ludwig, J. E. Spanier, M. Strokal, Y. Wada and Y. Wen, *Curr. Opin. Environ. Sustain.*, **36**, 59 (2019).
3. V. Ghaffarian, S. M. Mousavi, M. Bahreini and H. Jalaei, *J. Ind. Eng. Chem.*, **20**, 1359 (2014).
4. G. D. Kang and Y. M. Cao, *J. Membr. Sci.*, **463**, 145 (2014).
5. N. N. Li, A. G. Fane, W. W. Ho and T. Matsuura. John Wiley & Sons (2011).
6. A. Hai, A. A. Durrani, M. Selvaraj, F. Banat and M. A. Haija, *Sep. Purif. Technol.*, **212**, 388 (2019).
7. Y. C. Lin, K. M. Liu, P. L. Chiu, C. M. Chao, C. S. Wen, C. Y. Wang and H. H. Tseng, *J. Membr. Sci.*, **641**, 119874 (2022).
8. G. Moradi, S. Zinadini, L. Rajabi and S. Dadari, *Appl. Surf. Sci.*, **427**, 830 (2018).
9. M. Dmitrenko, A. Kuzminova, A. Zolotarev, D. Markelov, A. Komolkin, E. Loginova, T. Plisko, K. Burts, A. Bildyukevich and A. Penkova, *Sep. Purif. Technol.*, **286**, 120500 (2022).
10. D. Y. Zhang, Q. Hao, J. Liu, Y. S. Shi, J. Zhu, L. Su and Y. Wang, *Sep. Purif. Technol.*, **192**, 230 (2018).
11. J. Ali, E. Alhseinat, M. Abi Jaoude, I. M. Al Nashef, I. A. Adeyemi, T. M. Aminabhavi and H. A. Arafat, *Chem. Eng. J.*, **433**, 134596 (2022).
12. M. Khajouei, M. Najafi and S. A. Jafari, *Chem. Eng. Res. Des.*, **142**, 34 (2019).
13. K. Burts, T. Plisko, A. Bildyukevich, G. Rodrigues, M. Sjölin, F. Lipnizki and M. Ulbricht, *Colloids Surf. A: Physicochem. Eng. Asp.*, **632**, 127742 (2022).
14. N. Nasrollahi, S. Aber, V. Vatanpour and N. M. Mahmoodi, *Mater. Chem. Phys.*, **222**, 338 (2019).
15. V. Vatanpour and S. Paziresh, *J. Appl. Polym. Sci.*, **139**, 51428 (2022).
16. A. Dehban, A. Kargari and F. Z. Ashtiani, *Sep. Purif. Technol.*, **212**, 986 (2019).
17. S. Nara and H. T. Oyama, *Polym. J.*, **46**, 568 (2014).
18. S. Darvishmanesh, J. C. Jansen, F. Tasselli, E. Tocci, P. Luis, J. Degrève, E. Drioli and B. Van der Bruggen, *J. Membr. Sci.*, **379**, 60 (2011).
19. P. J. Jones, R. D. Cook, C. N. McWright, R. J. Nalty, V. Choudhary and S. E. Morgan, *J. Appl. Polym. Sci.*, **121**, 2945 (2011).
20. M. J. El-Hibri and S. A. Weinberg, in *Encyclopedia of polymer science technology*, John Wiley & Sons (2002).
21. A. Thanigaivelan, K. Noel Jacob and K. Rajkumar, *Int. J. Chemtech Res.*, **8**, 77 (2015).
22. P. S. Zhong, N. Widjojo, T. S. Chung, M. Weber and C. Maletzko, *J. Membr. Sci.*, **417**, 52 (2012).
23. T. Arumugham, N. J. Kaleekkal and M. Doraiswamy, *J. Appl. Polym. Sci.*, **132**, 41986 (2015).
24. M. V. Brami, Y. Oren, C. Linder and R. Bernstein, *Polymer*, **111**, 137 (2017).
25. L. L. Hwang, H. H. Tseng and J. C. Chen, *J. Membr. Sci.*, **384**, 72 (2011).
26. D. L. Arockiasamy, J. Alam and M. Alhoshan, *Appl. Water Sci.*, **3**, 93 (2013).
27. N. A. A. Sani, W. J. Lau, N. A. H. M. Nordin and A. F. Ismail, *Chem. Eng. Res. Des.*, **115**, 66 (2016).
28. Q. F. Alsalhy, J. M. Ali, A. A. Abbas, A. Rashed, B. V. d. Bruggen and S. Balta, *Desal. Water Treat.*, **51**, 6070 (2013).
29. Y. Feng, G. Han, T. S. Chung, M. Weber, N. Widjojo and C. Maletzko, *J. Membr. Sci.*, **531**, 27 (2017).
30. I. Moideen K, A. M. Isloor, A. Ismail, A. Obaid and H. K. Fun, *Desal. Water Treat.*, **57**, 19810 (2016).
31. S. Kiani, S. M. Mousavi, E. Saljoughi and N. Shahtahmassebi, *J. Polym. Adv. Technol.*, **29**, 1632 (2018).
32. J. Liu, Z. Zhong, R. Ma, W. Zhang and J. Li, *Membranes*, **6**, 35 (2016).
33. N. Ghaemi, S. S. Madaeni, A. Alizadeh, P. Daraei, V. Vatanpour and M. Falsafi, *Desalination*, **290**, 99 (2012).
34. S. Kiani, S. M. Mousavi, N. Shahtahmassebi and E. Saljoughi, *Desal. Water Treat.*, **57**, 16250 (2016).
35. E. Saljoughi, S. M. Mousavi and S. A. Hosseini, *Polym. Adv. Technol.*, **24**, 383 (2013).
36. N. Nikooe and E. Saljoughi, *Appl. Surf. Sci.*, **413**, 41 (2017).
37. Y. Ma, F. Shi, Z. Wang, M. Wu, J. Ma and C. Gao, *Desalination*, **286**, 131 (2012).
38. C. H. Lee, S. H. Chang, W. J. Chen, K. C. Hung, Y. H. Lin, S. J. Liu, M. J. Hsieh, J. H. S. Pang and J. H. Juang, *J. Colloid Interface Sci.*, **439**, 88 (2015).
39. S. Kiani, S. M. Mousavi, N. Shahtahmassebi and E. Saljoughi, *Appl. Surf. Sci.*, **359**, 252 (2015).
40. M. Afifi, H. A. Golestani, S. Sharifi and S. Kiani, *Desal. Water Treat.*, **52**, 57 (2014).
41. N. Jullok, S. Darvishmanesh, P. Luis and B. Van der Bruggen, *Chem. Eng. J.*, **175**, 306 (2011).
42. C. Zhao, X. Xu, J. Chen and F. Yang, *J. Environ. Chem. Eng.*, **1**, 349 (2013).
43. M. F. Sonnenschein, *J. Polym. Sci. B Polym. Phys.*, **41**, 1168 (2003).
44. X. Andrieu, T. Vicedo and C. Fringant, *J. Power Sources*, *54*, 487 (1995).
45. F. M. Noori and N. A. Ali, *Int. J. Appl. Innov. Eng. Manag.*, **3**, 459 (2014).
46. A. J. Kajekar, B. Dodamani, A. M. Isloor, Z. A. Karim, N. B. Cheer, A. Ismail and S. J. Shilton, *Desalination*, **365**, 117 (2015).
47. C. Mu, Y. Su, M. Sun, W. Chen and Z. Jiang, *J. Membr. Sci.*, **350**, 293 (2010).
48. C. Xu, W. Huang, X. Lu, D. Yan, S. Chen and H. Huang, *Radiat. Phys. Chem.*, **81**, 1763 (2012).
49. F. Meng, S. R. Chae, A. Drews, M. Kraume, H. S. Shin and F. Yang, *Water Res.*, **43**, 1489 (2009).
50. E. Saljoughi and S. M. Mousavi, *Sep. Purif. Technol.*, **90**, 22 (2012).